PERGAMON

Journal of Structural Geology 21 (1999) 85–96

JOURNAL OF STRUCTURAL GEOLOGY

Mechanism of exfoliation joint formation in granitic rocks, Yosemite National Park

Dov Bahat[a], Ken Grossenbacher[b], Kenzi Karasaki[b]

[a]*Department of Geological and Environmental Sciences, Ben Gurion University of the Negev, Beer Sheva 84105, Israel*
[b]*Earth Sciences Division, Lawrence Berkeley National Laboratory, 1 Cyclotron Road, Berkeley, CA 94720, U.S.A.*

Received 12 November 1997; accepted in revised form 11 June 1998

Abstract

Fractographic techniques reveal mechanical aspects of exfoliation in granitic rocks at Yosemite National Park, and electronic surveying provides information on their attitudes and dimensions. In the middle elevations of the cliff of El Capitan, exfoliation consists of early fractures a few meters to tens of meters in size which are fan-shaped. Fans at upper elevations point upwards, whereas fans at lower elevations point downwards parallel to the cliff. The fans interact with each other and merge into composite joints hundreds of meters in size, normal to the minimum compressive principal stress. This polarity indicates exfoliation by longitudinal splitting and buckling. The palaeostress causing the exfoliation on the southwestern side of Half Dome is estimated to range between 0.01 MPa and 0.94 MPa. Differences in fracture paleostresses of joints may be used in comparing their relative propagation velocities. It is suggested that the large exfoliation on the southwestern side of Half Dome had undergone a prolonged sub-critical growth before attaining rapid fracture velocities under post-critical conditions.

1. Introduction

1.1. Previous concepts on exfoliation mechanisms

The terms exfoliation and sheeting have been used interchangeably by various investigators (e.g. Holzhausen, 1989) and this terminology is followed in the present study. The origin of exfoliation in rocks has been debated since Gilbert's (1904) theory connecting sheeting with induced tension by the expansion of the rock body in response to erosion. Sheeting has been attributed to various causes, including local or regional compressive stresses imposed after crystallization, large-scale compression parallel to the exposed rock surface (Dale, 1923; Johnson, 1970; Twidale, 1973) and high differential stresses (White, 1946; Holzhausen, 1989). Various factors, including insulation, ground surface temperature fluctuations due to heating, cooling and frost, differential weathering, residual stresses and vegetation were considered related to the exfoliation processes (Johnson, 1970; Holzhausen, 1989). The maximum-principal-strain criterion predicts fracture by exfoliation joints normal to the direction of the maximum principal strain e_1 whenever the critical strain e_c is exceeded (Cadman, 1969; Johnson, 1970; Holman, 1976). Sheet fractures were interpreted to propagate in a principal stress plane, normal to the least principal compressive stress in the rock mass (Cadman, 1969; Holzhausen, 1989). The latter interpretation coincides with the concept that restricts joints to fractures that propagate normal to σ_3 (Engelder, 1985). Valuable information pertaining to the above mentioned mechanisms of sheeting was obtained on granites from New England (Jahns, 1943; Johnson, 1970).

1.2. Practical importance of exfoliation joints

Exfoliation reflects a general tendency of rock to fracture parallel to a previous topographic surface if stresses allow. Therefore, exfoliation is a significant consideration in road and dam construction and maintenance. Carefully planned excavation procedures, based on exfoliation data, can overcome some acute safety problems and avoid economic losses (Cadman, 1969; Holzhausen, 1989). Exfoliation fractures are central in some hydrological-environmental projects related to waste isolation and remediation, where

0191-8141/99 $ - see front matter
PII: S0191-8141(98)00069-8

accurate characterization of the fracture system is important (e.g. Cohen, 1993). Exfoliation on principal planes is not limited to flat planes. It also occurs parallel to curved surfaces, when stresses permit. Hence, this phenomenon is significant along tube-like structures such a tunnels and boreholes, because these types of openings suffer from unstable cracking parallel to newly created surfaces.

1.3. Geological setting at Yosemite National Park

The granitic rocks at Yosemite National Park constitute part of the Sierra Nevada batholith (Fig. 1). The 'monoliths' El Capitan and Half Dome are parts of the "intrusive suite of Yosemite Valley" (Huber, 1987). The El Capitan Granite intruded older plutons about 108 My ago and now makes up the bulk of the west half of the valley area. Dikes of the Taft Granite intruded the El Capitan (Huber, 1987). They commonly are lighter and finer grained than El Capitan Granite. Half Dome is composed of granodiorite.

Regional near-vertical fracture sets striking N–NW and E–NE and approximately perpendicular to each other are abundant in the Sierra Nevada batholith (Becker, 1891). Huber (1987, fig. 33) observed these two principal sets of joints in the Yosemite Valley area. The age of these joints is in debate. According to one view the joints formed during the emplacement of the plutons (e.g. Balk, 1937; Mayo, 1941) or soon after, between 85 and 79 Ma (Segall et al., 1990). Other investigators consider that the continuity of joints across boundaries between individual plutons indicates that the joints formed after the consolidation of the entire Sierra Nevada batholith. Becker (1891) suggested that the fractures are Pliocene in age, whereas Lockwood and Moore (1979) proposed that similar joints are post-Pliocene. According to Huber (1987) jointing could have occurred during later tectonic events, such as tilting of the Sierra region, 25–15 My ago. He suggested that the vertical cliffs of Yosemite may have hidden vertical fractures behind and parallel to the cliff face. In that case, vertical exfoliation possibly took advantage of free surfaces provided by previous jointing. Important studies on exfoliation in granitic rocks in Yosemite National Park were also carried out by Cadman (1969) and Holman (1976).

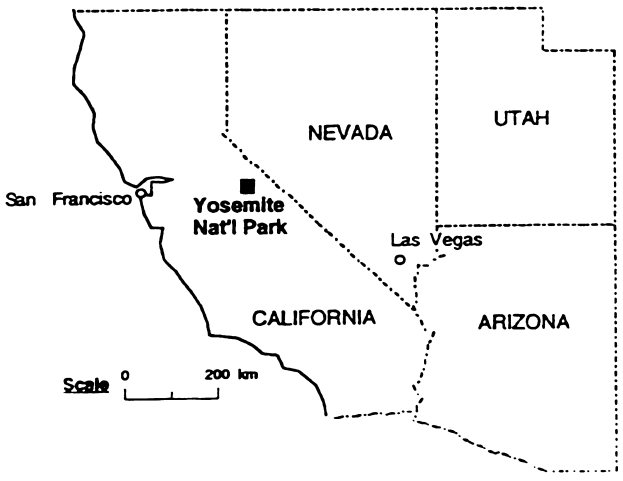

Fig. 1. Map showing the location of Yosemite National Park.

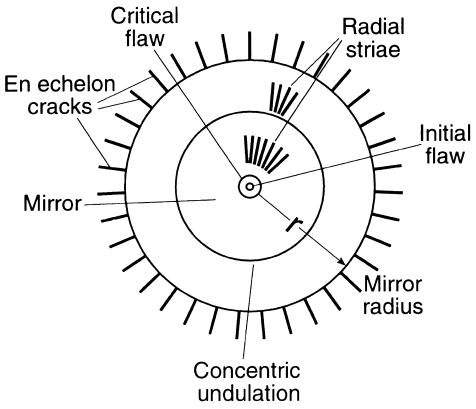

Fig. 2. Schematic representation of a fracture surface showing various fractographic elements (modified after Bahat, 1979). The mirror radius, r (arrow) is measured from the critical flaw to the inner boundary of the rim of en échelon cracks (not scaled).

1.4. Objectives

The present research concerns both qualitative and quantitative fractographic and electronic surveying methods applied to the fracture surface morphologies of exfoliation joints on the cliffs of El Capitan and the southwestern side of Half Dome. The aims of this investigation are to estimate the magnitude of the paleostresses that created a particular exfoliation joint, to establish the mechanism leading to exfoliation and to evaluate relative fracture velocities of joints.

2. Methods

2.1. Fracture surface morphology

Fracture initiates in the rock at stress concentrators. The fracture then propagates through a great number of disturbances caused by material heterogeneities, interfering stresses and emanating sound waves. These disturbances interact with the advancing fracture front and the results are recorded on the fracture surface by characteristic fracture surface morphology, also termed fracture markings (Kerkhof, 1973).

Fractography is a method for the analysis of fracture surface morphology to determine the mechanisms of fracture propagation and the causative stresses

involved in the process. Tectonofractography applies fractographical analysis to rock fracture with the objective of identifying and determining the necessary mechanical conditions and the tectonophysical processes that produced the fracture.

A fracture surface exhibits characteristic morphological features (Fig. 2) including the fracture origin at an initial flaw, which develops to a larger, critical flaw from which unstable fracture may occur. These flaws occur together with plumes (which are made of radial striae or barbs), concentric undulations (rib marks), and Wallner lines in the mirror plane. En échelon cracks form rims around the mirror plane. The distance between the origin to the rim is the mirror radius, which may be used to estimate the fracture stress. Explanations of the various fracture markings have been suggested by various investigators (e.g. Woodworth, 1895; De Freminville, 1914; Hodgson, 1961; Bankwitz, 1965; Kulander et al., 1979; Pollard et al., 1982; Bahat, 1991).

Undulations develop by local mixed modes II + I due to stress fields that progressively bend the crack front around the axis normal to the direction of propagation when both axes are on the fracture surface. En échelon segmentation essentially follows the rules leading to the formation of plumes. Both markings form by local mixed modes III + I in a stress field which rotates the fracture front about the axis of the direction of crack propagation (Preston, 1931; Sommer, 1969; Lawn and Wilshaw, 1975). Whereas the plume develops within the mirror, en échelon segmentation occurs beyond the mirror boundaries (Fig. 2), suggesting differences in stress intensity conditions (Bahat, 1991, p.191). Hertzberg (1976, fig. 14.9) shows a mirror plane with radial plumes surrounded by a rim of en échelon segments. This mirror resulted from a fatigue test (slow fracture propagation) on a steel turbine rotor (Yukawa et al., 1969). However, unstable conditions (rapid propagation) could have been attained at late stages of the fracture. The well defined fractography of the turbine rotor mentioned above (particularly, the sharp rim boundary) provided Hertzberg with a good basis for fracture mechanics calculations. The relevance of changes in propagation velocities of a given fracture to geological structures is further discussed below.

Although fractographic techniques have been widely used in investigating jointing in general, they rarely have been applied to sheet fracture. Holman (1976) and Holzhausen (1989) studied fracture markings in exfoliated granites. Holzhausen (1989) pointed out the importance of these markings, particularly regarding the significance of the en échelon segmentation on granitic sheet surfaces, and suggested that exfoliation may form by rapid unstable propagation. Bahat (1991, p. 149 and 234) showed fracture markings on a sheet joint in chalk and correlated these features to differences in stress intensity parameters by making the distinction between plumes and hackles.

2.2. Electronic surveying

An electronic total station, which incorporates a laser range-finder, provided the means to survey the cliffs at Yosemite National Park (see also Grossenbacher et al., 1996). A principal assumption in this technique is that the cliff is flat, which applies to the investigated exfoliation joints. For the geometries used, a deviation of 3 m from flatness yields an error in calculated position on a cliff of at most 1 m. This does not appear to be a problem, as the relief on the cliff is less than 5 m (as verified by examination of topographic base maps), with distances measured of about 50–100 m, and distance from base station to cliff of over 300 m. Taken together, these yield an error of less than 3%, which was deemed acceptable, considering the large distances in the park and the range of estimated paleostress magnitudes involved (see below).

3. Descriptive fractography and estimation of fracture paleostress on exfoliation joints

Fractures were studied at El Capitan Granite and at the Half Dome Granodiorite in Yosemite National Park. Qualitative fractography was investigated on the cliffs of El Capitan and Half Dome, and quantitative research was carried out on the latter, where the boundary of a mirror plane is well exposed for paleostress calculations.

3.1. Fracture morphology at the middle height of the cliff of El Capitan

Exfoliation surfaces were examined in the middle height of the approximately 1000 m high granitic cliff of El Capitan, within the frame shown in Fig. 3(a). Vertical fracture surfaces on the N 32°E oriented exfoliations are marked by tens of early cracks which are shaped as fans. Each fan is comprised of an origin and radial plumes. Occasionally, a single concentric undulation, or more than one undulation (Fig. 3a and b) form orthogonal relationships with the plumes at their intersections on the fans. Distorted fans, manifested by plumes deviating from a radial pattern are common as well. The size of a fan varies from several meters to several tens of meters. Occasionally, only partially developed radial plumes appear.

These fans cut country-rock and dikes of the Taft Granite (Fig. 3b) without apparent change in direction. Early circular cracks, resembling in shape and

size similar fractures from Zion National Park (Bahat et al., 1995) also occur sporadically on the cliff of El Capitan. The fans are by far more common than the early circular cracks. Many neighboring fans interacting with each other merge into composite vertical joints which are several hundreds of meters in size.

The fan population produces a specific fracture pattern at the middle height of the cliff. This pattern is not so clear for fractures A and B (Fig. 3c). On the other hand, a particular preferred orientation appears for fractures C and D. On the latter two fractures, fans indicate upward propagation above the approximate height of D (where undulations in the fans convex upward), and fans below this height show downward propagation (where undulations in the fans convex downward). Hence, fans cutting the granite at El Capitan propagated upward and downward from initiation zones on individual exfoliations. These zones occupy similar heights on the cliff (Fig. 3d).

A few exfoliation joints occur parallel to each other on the cliff, such that each pair of adjacent joints contain a rock 'slice' between them which is sub-parallel to the cliff. Some of the slices do not maintain a constant thickness, causing deviations from parallelism of the exfoliation joints. Letters A–D in Fig. 3(c) represent surviving remnants of distinct exfoliation surfaces, such that D reveals that the previous more external slices (A–C) have been removed at this location. Exfoliated slices apparently detach selectively from the cliff in a gravity driven process, as revealed by certain undetached parts from the cliff (see dashed lines in Fig. 3c).

3.2. Two superposing exfoliation fractures on the Half Dome granodiorite

An exfoliation joint striking N 27° E and dipping 42° NW on the southwestern side of Half Dome (Fig. 4a), reveals the approximate location of its fracture origin at the meeting area of the distorted radial barbs of a large plume (P in Fig. 4b). Part of an external slice which had existed above this joint was removed by erosion, leaving behind a concentric rim of radial en échelon cracks which had circled the mirror plane of the removed joint. The extrapolated merger of the en échelon segments on the removed slice would occur on its right side, implying opposite directions of fracture propagation in the two superposing

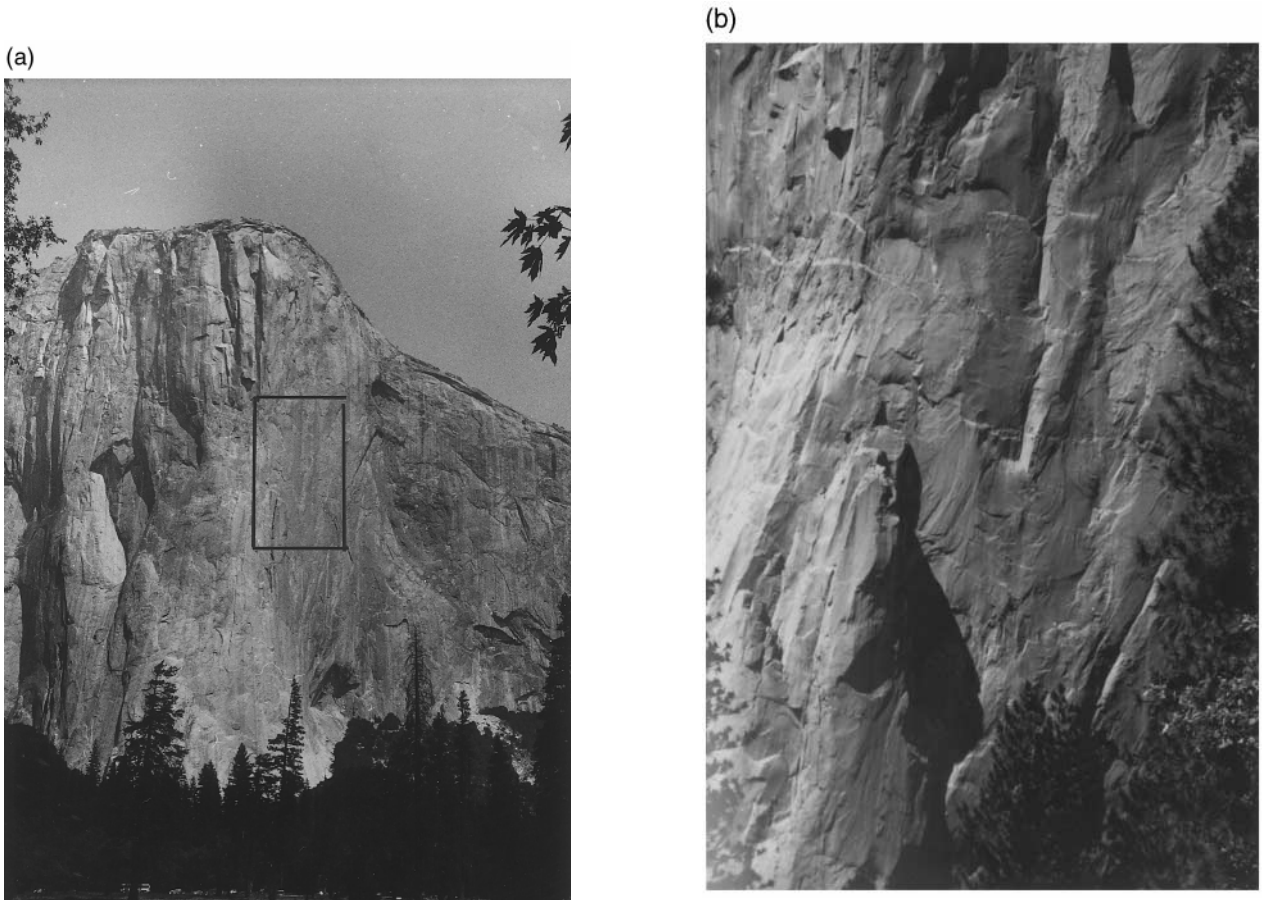

Fig. 3(a,b).

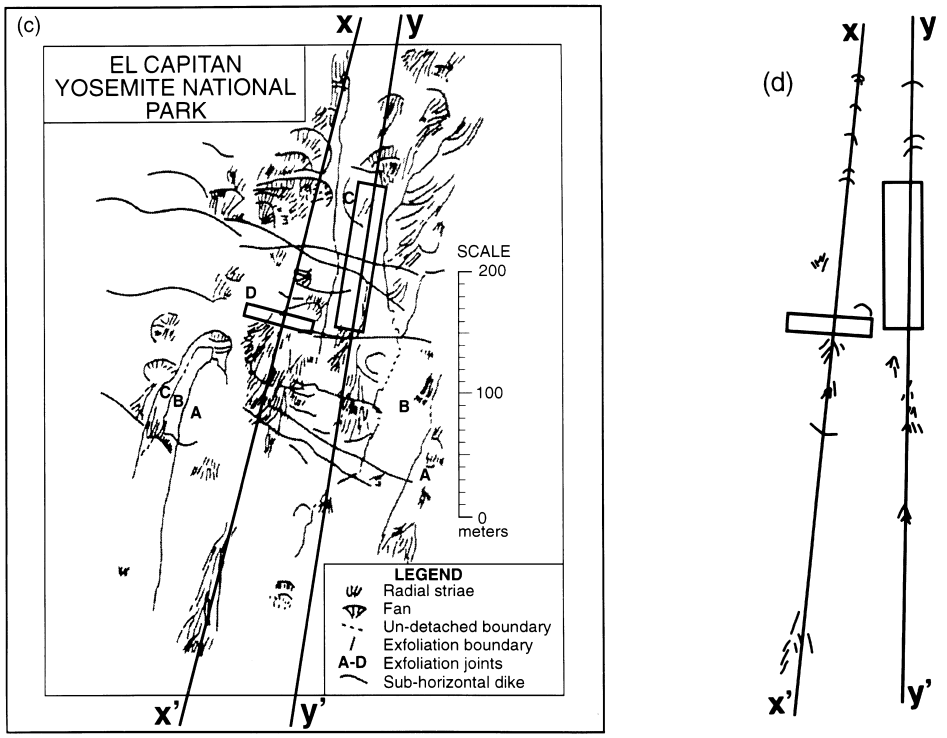

Fig. 3. Exfoliating joints in the El Capitan Granite at Yosemite National Park. (a) Photograph of a cliff on El Capitan striking N 32°E, showing area further detailed in (b). (b) Photograph of the exfoliated cliff within the frame outlined in (a), showing multiple groups of radial striae. Some groups occur in association with concentric undulations, together forming fan-shapes. The cliff is divided by sub-vertical fractures into distinct exfoliations. Fractures cut sub-horizontal dikes of the Taft Granite (which have a light color). (c) Scaled diagram of (b) showing exfoliation boundaries between slices belonging to distinct joints A–D. Rectangles designate initiation zones at which the propagations depart to opposite directions, as shown by traces of convexed undulations or radial plumes. (d) Traverses x–x' and y–y' on joints C and D from (c) depicting fans. The fans are either radiating barbs or convexed undulations pointing to the direction of fracture propagation upwards in the upper part of diagram, and downwards in the lower one. Rectangles as in (c).

exfoliation joints and indicating independent propagations of adjacent exfoliation joints. The large plume (Fig. 4a and b) represents a joint that grew from a single nucleation origin, resembling some of the fans on the cliff of El Capitan (Fig. 3).

3.3. Estimation of the tensile fracture stress on the exfoliation joint from Half Dome

3.3.1. General remarks

One way of establishing the mechanism of exfoliation is by estimating the fracture stress σ_f for the development of individual fractures. As mentioned above, exfoliation is generally thought to be a consequence of tensile fracturing that propagates parallel to high compressive stresses, but this needs to be quantitatively verified. Fractography is a useful technique for this task.

Three questions are considered within the framework of physical constraints when applying fractographic techniques to geological problems: first, can we apply observations from ceramics to mechanical calculations in rocks? Second, are values of fracture toughness (K_{Ic}), experimentally obtained for finite sample sizes, valid as material property for rocks under geological loading conditions. Third, can we use the en échelon rim in our calculation?

The answers to these questions are positive. Fracture mechanic results derived from polymers suggest analogies to fracture in rocks (Cooke and Pollard, 1996), so that the affinity between two groups of polycrystalline materials (silicate ceramics and granitic rocks) is acceptable. Furthermore, K_{Ic} estimates derived from geological measurements are compatible with existing data from laboratory fracture experiments (Segall and Pollard, 1983). The concave side of the en échelon rim on the remnant of the removed slice has quite a sharp boundary (Fig. 4a and b). This suggests, in analogy to similar fractures in technological materials (see above mentioned study by Herzberg, 1976) that the fracture stress, σ_f can be estimated on the joint relict from the southwestern side of Half Dome.

We applied two methods which relate to the basic fracture mechanic equation $K = \sigma\sqrt{\pi}\sqrt{C}$, where K is the stress intensity factor, σ is the applied stress, and C

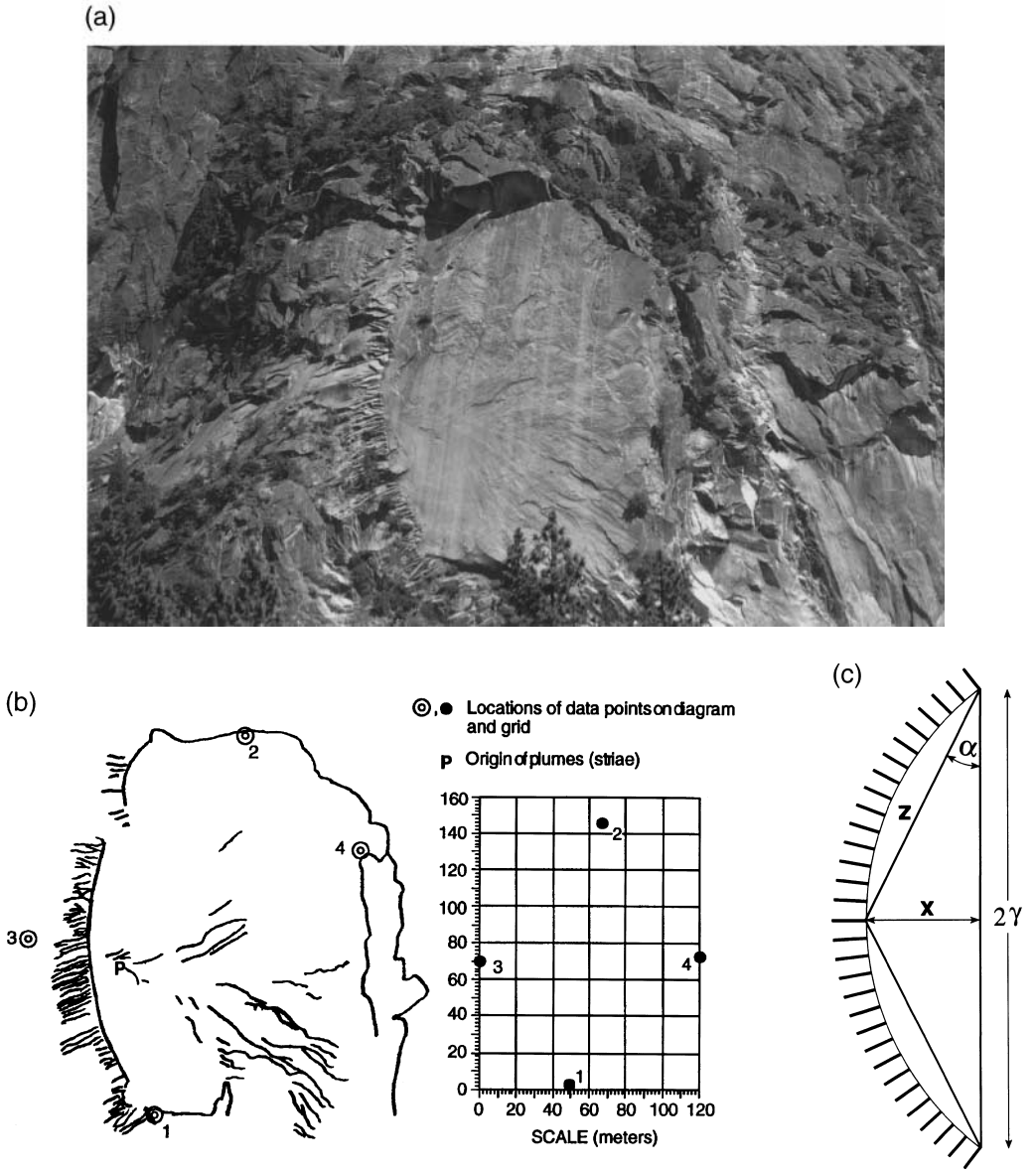

Fig. 4. Exfoliation joints striking N 27°E and dipping 42°NW on the southwestern side of Half Dome at Yosemite National Park. (a) Photograph of a concentric rim of en échelon cracks at left representing a remnant of an exfoliation joint on a slice which has been removed. (b) Scaled diagram and grid of (a). The removal of the external slice exposed the surface of a second exfoliation joint whose origin is identified at P by the meeting area of radial barbs of a large plume. (c) Diagram showing the curved inner boundary of the rim of en échelon cracks and the angle α between $2y$ and z, for the calculation of mirror radius.

is half depth of the crack (Irwin, 1962). These two methods however, require different parameters for the calculation (Bahat and Rabinovitch, 1988), as shown below.

3.3.2. The stress intensity method

We calculated σ_f on the basis of the empirical relationship (Randall, 1966):

$$\sigma_f = K_{Ic}[Q/(1.2\pi C_{cr})]^{1/2} \quad (1)$$

where K_{Ic} is the critical stress intensity factor (the fracture toughness), Q is the modifying geometrical factor and C_{cr} is the radius of the critical flaw. Values of K_{Ic} vary considerably for different granitic rocks, reflecting rock properties and experimental techniques performed by different investigators. Since we do not have data on the fracture toughness of the Half Dome granodiorite, we applied in the calculation the two extreme K_{Ic} values in the range from 0.04 MPa $m^{1/2}$ to 4.6 MPa $m^{1/2}$ obtained by Segall and Pollard (1983) for Mount Givens Granodiorite in the Sierra Nevada. The Q factor ranges in value from 1.0 for a long shallow flaw to 2.46 for a semi-circular flaw (Randall, 1966). Since the shape of the flaw was not known, we used both values in the calculation.

The location of the fracture origin is uncertain, so that the mirror radius, r (Fig. 2) needs to be determined trigonometrically. The measured distances were (Fig. 4c): $2y$ between the two tips of the visible rim and x. We used the relationships $z/\sin\alpha = 2r$, where α is the angle produced by $2y$ and z; also, $z^2 = x^2 + y^2$ and $r = x^2 + y^2/2x$. For the derivation of r two distances where determined at random locations along the rim boundary resulting in two r values differing 8% from each other, suggesting the error range in measurement.

The error in r determination related to distance measurement and to a slight ellipticity deviation of the mirror from circularity is estimated as 15%. Accordingly, r was calculated to be 96.4 ± 7.7 m. We derived the radius of the critical flaw C_{cr} from r/C_{cr} = constant. This is an acceptable constant for fracture mirrors of many glasses and ceramics, and it varies from 13.9 to 16.7 (Mecholsky and Freiman, 1979). Therefore we assume its relevance to rocks. We used for this ratio the mean value $r/C_{cr} = 15.3$, and obtained $C_{cr} = 6.3$ m. There is no need to calculate the two extremes which vary only insignificantly from each other when applied to Eq. (1). The results for σ_f range from 0.01 MPa to 1.48 MPa (Table 1).

3.3.3. The surface energy method

For the calculation of σ_f, we applied the expression (Congleton and Petch, 1967):

$$\sigma_f = 2G(E\gamma/\pi r)^{1/2} \quad (2)$$

where E is Young's modulus, γ is surface energy, r is the radius of the mirror plane and G is the enhancement factor which varies from $2\sqrt{2}$ to $5\sqrt{2}$. The component $\sqrt{2}$ of the G factor relates to the position of the Griffith crack with respect to the tip of the parent fracture (almost insignificant in this case); and the change in the range 2–5, is a function of the strain rate ahead of the parent fracture. An increase in the fracture velocity would favor the upper end of this range (Congleton and Petch, 1967). We calculated σ_f for the two extreme values of G, 2.8284 and 7.0711. We used $E = 5.0 \times 10^{10}$ Pa as the Young's modulus of granodiorite (Segall and Pollard, 1983). Both $\gamma = 4.06$ J m^{-2} the fracture surface energy for microcline (Atkinson and Avdis, 1980), and $\gamma = 0.69$ J m^{-2} the fracture surface energy for Japanese granite (Atkinson and Meredith, 1987) were applied in the calculation. The results for σ_f range from 0.06 MPa to 0.37 MPa (Table 1).

The results obtained by the surface energy method fall well within the range of the two middle results derived by the stress intensity method (0.06–0.37 MPa and 0.01–0.94 MPa, respectively). We therefore suggest that the range 0.01–0.94 MPa is a good estimate of σ_f. However, the surface energy method is considered to be more reliable than the stress intensity method, because it relates directly to the mirror radius. Therefore, we do not rule out the possibility that the range 0.06–0.37 MPa is a better representative of σ_f.

4. Mechanism of exfoliation during the initiation and propagation stages in the middle height of El Capitan cliff

According to Holzhausen and Johnson (1979) longitudinal splitting occurs parallel or sub-parallel to the direction of loading in uniaxially compressed rock cylinders. Although longitudinal fracture often originates at the ends of the specimens (due to sample end-effects) and propagates toward the center, uniform

Table 1
Estimation of fracture stress σ_f on exfoliation joints from Half Dome at Yosemite National Park (southwestern side)

The stress intensity method				
K_{IC} (MPa m$^{1/2}$)	Q	C_{cr} (m)		σ_f (Mpa)
0.04	1.00	6.30		0.01
4.60	1.00	6.30		0.94
0.04	2.46	6.30		0.01
4.60	2.46	6.30		1.48
The surface energy method				
G-factor	E ($\times 10^{10}$ Pa)	γ (Jm^{-2})	r (m)	σ_f (MPa)
2.8284	5.000	4.06	96.4	0.15
7.0711	5.000	4.06	96.4	0.37
2.8284	5.000	0.69	96.4	0.06
7.0711	5.000	0.69	96.4	0.15

Terms used are: The critical stress intensity factor (the fracture toughness) K_{Ic}, the modifying geometrical factor Q, the radius of the critical flaw C_{cr}, the fracture stress σ_f, the enhancement factor G, Young's modulus E, the fracture surface energy γ and the mirror radius r.

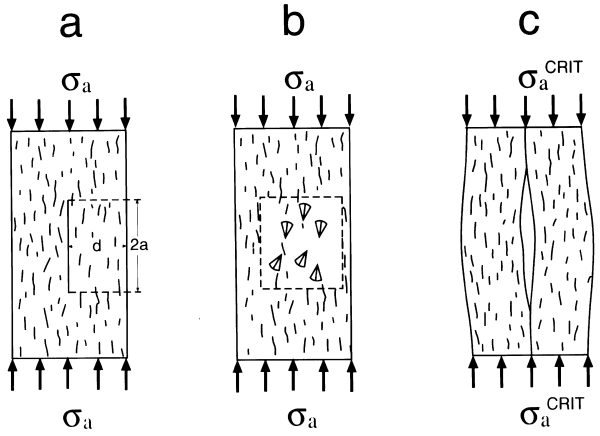

Fig. 5. Schematic representation of how buckling causes longitudinal splitting of cylindrical specimens. (a) Axial cracks coalesce under applied stress σ_a to an 'internal fracture' of length $2a$ at a distance d from the free surface. (b) The internal fracture shown at 90° position to (a) exhibiting early cracks in shapes of fans pointing upward and downward before coalescence. (c) Axial propagation of the internal fracture (in the a position) occurs when it buckles outward (modified after Holzhausen and Johnson, 1979).

loading also results in fracture origins within the specimens (Peng, 1970). Holzhausen and Johnson (1979) postulate that an 'internal fracture' is formed by the coalescence of earlier axial cracks (analogous to the term composite fracture used in the present study) which have been created under high loads (Fig. 5a and b). An extension of the internal surface to longitudinal splitting might be caused by buckling of the rock away from this surface, when the two separated parts of the cylinder bend outward (Fig. 5c). Tension at the tips of the longitudinal split may cause unstable growth to the ends of the specimen. Holzhausen and Johnson (1979) consider several tensile and shear criteria, but refrain from advocating one mechanism leading to splitting.

Our findings in the field fit quite well with various experimental observations made by Holzhausen and Johnson (1979). Coalescence of coplanar fans (Fig. 3b–d) which are close to and parallel to free surfaces (the outer surface of the cliff) is the main fracture process in the middle height of El Capitan cliff that leads to exfoliation. Exfoliation developed along principal planes populated by multiple early cracks, by a mechanism of longitudinal splitting which was caused by the overburden load. Splitting occurred upward and downward from an initiation zone, at an elevation where the normal resistance to buckling was minimal (Fig. 6), next to a free surface in analogy to Fig. 5. Fracture propagation on El Capitan cliff was polarized upwards and downwards from this zone. It followed the creation of multinucleation sites of independent cracks which had developed into fans and then merged with each other into composite joints (Fig. 3c and d).

Regarding the tension vs shear mechanisms causing the splitting, which were considered by Holzhausen and Johnson (1979), our fractographic observations strongly suggest that: (a) the undulations and plumes on the surfaces of the early joints reflect mode I opening as the predominant mode (Bahat, 1979), i.e. on principal planes normal to the minimum principal stress; (b) minor local shear was superposing the tensile mode (Bahat, 1987); (c) significant shear strain can be ruled out because such a process would have erased

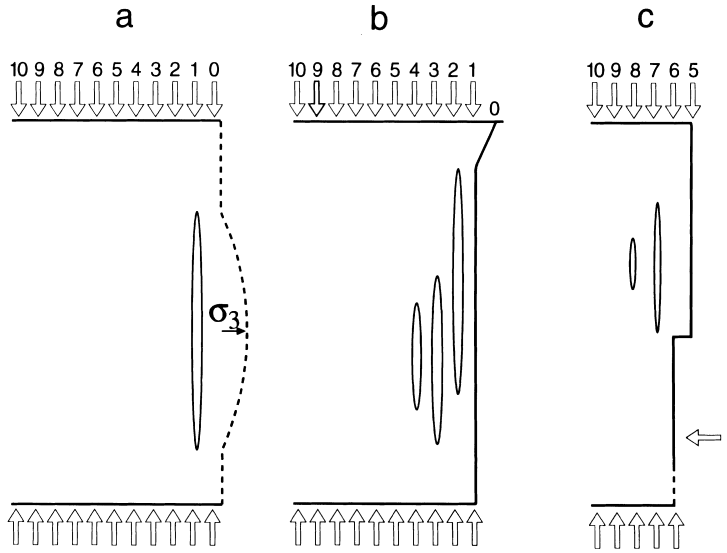

Fig. 6. A section model showing the profile of joint exfoliation by longitudinal splitting and buckling of the 'internal fracture' from Fig. 5(a). Vertical arrows indicate overburden load. Fracture (longitudinal splitting) occurs in association with buckling (an exaggerated buckling is shown by the dashed line) which develops sub-normal to σ_3 (horizontal arrow). (b) An early slice collapsed (at 0) and washed away, and new exfoliations develop (earlier ones closer to the free surface at arrow numbered 1 to arrow numbered 10). (c) A profile of an arch at the lower part of the cliff which forms when part of the slice collapses (white arrow).

the fracture markings, and (d) however, the lack of hackle (present terminology) or exfoliation-branching questions an unstable fracture analogous to that observed experimentally (Holzhausen and Johnson, 1979). Our observations suggest stable joint propagation in the middle height of El Capitan cliff, that may be correlated with the compressive state in the uppermost lithosphere (this topic is further elaborated below).

We adapt the formula used by Holzhausen and Johnson (1979) to analyze the critical conditions for buckling:

$$\sigma_a^{crit}/(\pi^2 E/3) = (d/2a)^2 \quad (3)$$

where σ_a^{crit} is the critical axial stress for buckling of a beam with fixed ends, E is Young's modulus, d is the distance between the internal surface (nucleation of the longitudinal split) and the free surface, and $2a$ the internal surface length (Fig. 5). This formula shows that σ_a^{crit} increases with d^2. It explains the observations both in granite and in sandstone (Bahat et al., 1995) that vertical streaks produced by dripping solutions mark external exfoliations and do not mark internal ones. That is, the earlier longitudinal splits develop close to the free surface at small d values (Fig. 6); and then new ones gradually form from further inside the rock. Also, Eq. (3) implies that rock slices produced between successive exfoliations should be much thinner than the lengths of the associated 'internal fractures'. This may explain the great ranges of exfoliation spacings depicted in various publications (e.g. Holman, 1976, p. 2; Twiss and Moores, 1992, fig. 3.5). It appears that buckling can be promoted by only slightly developed internal fractures close to sub-horizontal ground surfaces of granites.

Joints are classified into four fracture categories, burial, syntectonic, uplift and post-uplift groups (Bahat, 1991; Engelder et al., 1993; Bankwitz and Bankwitz, 1994). These four groups differ in their various properties, including their fractographies. It turns out that the merger of early circular cracks and early fans is common to exfoliation joints in both granite and sandstone (Bahat et al. 1995). These are characteristic fractographic features exclusive to post-uplift joints which develop close to a 'free boundary' above the ground surface. A similar merger of fans into a larger post-uplift joint has been observed in chalk (Bahat, 1991, p. 301). Mergers of early circular cracks or early fans which occur on post-uplift joints are not known from surfaces of burial and uplift joints, and they are rare on syntectonic joints (Bahat, 1991).

What were these free boundaries? As mentioned above Huber (1987) suggested that the vertical exfoliations possibly took advantage of free surfaces provided by previous jointing. Our observations support his suggestion (Figs. 5 and 6). As mentioned in the introduction the previous joints could be related to various tectonic processes. Hence, exfoliation fractures are inferred to form under unloading conditions, and they differ from joints that are associated with burial or tectonic processes which generally occur under increasing loading.

5. Velocity of fracture propagation

Fan markings on exfoliation surfaces which cut the El Capitan Granite at Yosemite National Park are made of radial plumes and concentric undulations orthogonal to each other at their intersections, which implies contemporanity. This fracture morphology suggests a sub-critical propagation rate below 4×10^{-5} m/s, assuming dry conditions, and below 10^{-2} m/s, if the fracture were immersed in water (Bahat, 1991, p. 234). Accordingly, it would take longer than 14 days to fracture a fan having radial plumes 50 m long, in dry conditions, and a fan immersed in water, whose plume is 36 m long would fracture in more than an hour. Due to the uplift of the El Capitan block the middle height of the cliff is expected to be above the water table. In addition, due to the low porosity of the granite the above dry conditions are preferred. If however, splitting and buckling would enable water flow into the fracture zone, a more rapid fracture would occur. This would require a much stronger preference of downward fracture propagation compared with an upward propagation, due to the flow of more water towards lower elevations. This is not supported by the fan pattern in Fig. 3 (c and d) so that propagation under dry conditions is favored. Olson's (1993) calculations for joints from Sierra Nevada granites (generated by a mechanism other than exfoliation) suggest that fractures of some 10 m long were formed in about 3 min or faster.

The transition between sub-critical to post-critical fracture propagation is determined by the critical stress intensity factor K_{Ic} taken as that value of K_I needed to drive the crack. Following Wiederhorn et al. (1974) this occurs at a velocity of $\geqq 10^{-1}$ m/s. According to this criterion the exfoliation velocity on El Capitan cliff was sub-critical, whereas the fractures analyzed by Olson possibly propagated under conditions approaching critical.

The calculated tensile paleostresses that initiated joints in granitic rocks under three different geological conditions are presented in Table 2. The results compared here were obtained by different procedures. Whereas the present method is based on measuring fracture markers on surfaces of individual joints [and was applied to the analysis of fractures in the granodiorite from Yosemite Valley (this paper) and in the

Table 2
Tensile paleostress conditions for jointing in granodiorite and in granite

Post-uplift exfoliation joint in granodiorite from the SW cliff of Half Dome in Yosemite Valley, California		Relative fracture velocities*
The stress intensity method		
Range of fracture stress σ_f	0.01 to 1.48 MPa	Long growth under sub-critical conditions, and short post-critical growth
The surface energy method		
Range of fracture stress σ_f	0.06 to 0.37 Mpa	
Syntectonic joints in Granodiorites from Mt Givens (Segall and Pollard, 1983)		
Ward Lake	Florence Lake	Long growth under close to critical conditions, but never reaching them
Initial stress $\sigma_i \leq 26 \pm 11$ MPa	10 ± 6 Mpa	
Initial stress $\sigma_i \geq 1.7 \pm 0.9$ MPa	1.2 ± 1.0 Mpa	
Uplift joint in Granite from East Sinai (Bahat and Rabinovitch, 1988)		
The stress intensity method		
Range of fracture stress σ_f	2.9 to 15.8 MPa	Relatively short growth under sub-critical conditions before assuming post-critical growth
The surface energy method		
Range of fracture stress σ_f	2.4 to 6.0 Mpa	

* See text for discussion.

granite from East Sinai, by Bahat and Rabinovitch (1988)], the method used by Segall and Pollard (1983) relies on measurements of extension strain accommodated by the dilation of many joints (and was used for the analysis of fracture in granodiorites from Mt Givens). Accordingly, these two methods pertain to local and remote stresses, respectively.

Considering the relatively low overburden constraints, it is rather surprising that the σ_f result causing exfoliation on the southwest side of Half Dome was so low (ranging from 0.01 to 1.48 MPa). However, this result corresponds well with the qualitative fractographic observations from the middle height of El Capitan cliff which imply slow fracture propagation under low tensile stresses. For some reason, quite possibly fracture in dry rock, post-uplift exfoliation on large cliffs is mostly a slow process.

Segall and Pollard (1983) assumed quasi-static crack propagation conditions in their analysis of the initial tensile stresses for regional joints in the Mt Givens Granodiorite from the Sierra Nevada. The relatively high σ_f values resulting in jointing at Mt Givens (ranging from 1.2 ± 1.0 MPa to 26 ± 11 MPa) seem to suggest syntectonic fracture (Bahat, 1991) which was enhanced by pore pressure, as testified by mineral fillings (Segall and Pollard, 1983), but under considerable depths, that prevented fracture branching (Segall and Pollard, 1983). Such conditions would fit sub-critical fracture velocities (Table 2).

Greater fracture stress results than those mentioned above for the granodiorites were obtained for an uplift joint in a granite from Sinai (Bahat and Rabinovitch, 1988). The latter paleostress results are less but comparable to those obtained by tensile experiments on granite (from 7 MPa to 18 MPa, Segall and Pollard, 1983). Quite possibly, the Sinai joint started to propagate from certain depths below the water table while being exposed to excessive pore pressures that resulted in high σ_f values.

In summary, fracture velocities may change very considerably during the fracture process. We generally assume double stage processes in the three granitic rocks: (a) sub-critical fracture growth which had occurred before critical conditions were attained; and then, (b) post-critical fracture velocities that could have initiated under reduced overburden pressures (Bahat and Rabinovitch, 1988). The difference is in the amount of time for fracture growth during the first stage. The results suggest that the first stage was relatively long for the exfoliation in the cliff of Half Dome, whereas for the joint in East Sinai this stage was relatively short. Most joints, possibly including the joints from Mt Givens, never reach the second stage, mostly because of overburden constraints.

6. Conclusions

Fractographic techniques reveal new aspects of exfoliation in granitic rocks at Yosemite National Park. Detailed measurements carried out on exfoliation surfaces by outcrop inspection and electronic surveying provide information on their dimensions, attitudes and mechanisms of formation.

In the middle elevations of the cliff, exfoliations consist of early fan-shaped cracks. These fans consist of plumes and occasional concentric undulations and range in size from a few meters to tens of meters.

The fans interacted with each other and merged into composite fractures that further developed to exfoliations hundreds of meters in size, on planes normal to the minimum principal stress. The orientation of the

fans indicates that they initiated in nucleation zones at certain heights, from where they propagated upwards and downwards parallel to the cliff.

Exfoliation developed by the mechanisms of longitudinal splitting and buckling. This is strongly supported by the orientation polarity of fans on El Capitan cliff, pointing upwards and downwards.

The palaeostress σ_f causing the exfoliation in Half Dome is estimated to range from 0.01 MPa to 1.48 MPa by the stress intensity method and to range from 0.06 MPa to 0.37 MPa by the surface energy method. The reasonable overlap of the results by the two methods, particularly at the lower ends of the range suggests that they are reliable.

These are low fracture stress results for granitic rocks, suggesting a sub-critical process during most of the fracture process. However, a rapid fracture could have developed towards the end of the joint propagation.

Acknowledgements

This work was carried out under U.S. Department of Energy Contract No. DEAC03-76SF00098 for the Director, Office of Civilian Radioactive Waste Management, Office of External Relations, and was administered by the Nevada Operations Office, U.S. Department of Energy. This work was also partially supported by the Power Reactor and Nuclear Fuel Development Corporation of Japan. We thank Sally Benson, Bo Bodvarsson, and Paul Witherspoon for their facilitation of the project. Special thanks are due for Pascual Benito for his work on the figures. Finally, we wish to thank David Peacock, Stephen Laubach, Patience Cowie, an unnamed referee, Richard Lisle and Chaim Benjamini for their thoughtful and detailed reviews of our material.

References

Atkinson, B.K., Avdis, V., 1980. Fracture mechanics parameters of some rock forming minerals determined using an indentation technique. International Journal of Rock Mechanics and Mining Sciences & Geomechanics Abstracts 7, 383–386.

Atkinson, B.K., Meredith, P.G., 1987. Experimental fracture mechanics data for rocks and minerals. In: Atkinson, B.K., (Ed.), Fracture Mechanics of Rocks, Academic Press, London.

Bahat, D., 1987. Correlation between fracture surface morphology and orientation of cross-fold joints in Eocene chalks around Beer Sheva, Israel. Tectonophysics 36, 323–333.

Bahat, D., 1979. Theoretical considerations on mechanical parameters of joint surfaces based on studies on ceramics. Geological Magazine 11, 81–92.

Bahat, D., 1991. Tectonofractography. Springer-Verlag, Heidelberg.

Bahat, D., Rabinovitch, A., 1988. Paleostress determination in a rock by fractographic method. Journal of Structural Geology 10, 193–199.

Bahat, D., Grossenbacher, K., Karasaki, K., 1995. Investigation of exfoliation joints in Navajo sandstone at the Zion National Park and in granite at the Yosemite National Park by tectonofractographic techniques. Lawrence Berkeley Laboratory, 36971.

Balk, R., 1937. Structural behavior of igneous rocks. Geological Society of America Memoir.

Bankwitz, P., 1965. Uber klufte 1. Beobachtungen im Thuringischen Schiefergebirge. Geologie 14, 241–253.

Bankwitz, P., Bankwitz, E., 1994. Event related jointing in rocks on Bornholm island (Denmark). Zeitschrift für Geologische Wissenschaften, 22, 97–114.

Becker, G.F., 1891. The structure of a portion of the Sierra Nevada of California. Geological Society of America Bulletin 2, 49–74.

Cadman, J., 1969. The origin of exfoliation joints in granitic rocks. Unpublished Ph.D. thesis. University of California, Berkeley, U.S.A.

Cohen, A. J. B., 1993. Hydrogeologic characterization of a fractured granitic rock aquifer, Raymond, California, pp. UC–400. Lawrence Berkeley Laboratory, 34838.

Congleton, J., Petch, N.J., 1967. Crack branching. Philosophical Magazine 16, 749–760.

Cooke, M.L., Pollard, D.D., 1996. Fracture propagation paths under mixed mode loading within rectangular blocks of polymethyl methacrylate. Journal of Geophysical Research 101, 3387–3400.

Dale, T.N., 1923. The commercial granites of New England. U.S. Geological Survey Bulletin 738.

De Freminville, M. Ch, 1914. Recherches sur la fragilité-l'éclatement. Revue de Métallurgie 11, 971–1056.

Engelder, T., 1985. Loading paths to joint propagation during cycle: an example of the Appalachian Plateau, USA. Journal of Structural Geology 7, 459–476.

Engelder, T., Fischer, M.P., Gross, M.R., 1993. Geological aspects of fracture mechanics, a short course manual notes. Geological Society of America Annual Meeting, Boston.

Gilbert, G.K., 1904. Domes and dome structures of the high Sierra. Geological Society of America Bulletin 15, 29–36.

Grossenbacher, K., Bahat, D., Karasaki, K., 1996. Triangulator: Excel spreadsheets for converting relative bearings to XYZ coordinates, with applications to scaling photographs and orienting surfaces. Computers and Geosciences 22, 1053–1059.

Hertzberg, R. W., 1976. Deformation and Fracture Mechanics of Engineering Materials. Wiley, New York.

Hodgson, R.A., 1961. Classification of structures on joint surfaces. American Journal of Science 259, 493–502.

Holman, W. R., 1976. The origin of sheeting joints. A hypothesis. Unpublished Ph.D. thesis. University of California, Los Angeles, U.S.A.

Holzhausen, G.R., 1989. Origin of sheet fracture, 1. Morphology and boundary conditions. Engineering Geology 27, 225–278.

Holzhausen, G.R., Johnson, A.M., 1979. Analyses of longitudinal splitting of uniaxially compressed rock cylinders:. International Journal of Rock Mechanics and Mining Sciences & Geomechanics Abstracts 16, 163–177.

Huber, N.K., 1987. The geologic story of Yosemite National Park. U.S. Geological Survey Bulletin 1595.

Irwin, G.R., 1962. Crack-extension force for a part-through crack in a plate. Journal of Applied Mechanics 29, 651–654.

Jahns, R.H., 1943. Sheet structure in granites: its origin and use as a measure of glacial erosion in New England. Journal of Geology 51, 71–98.

Johnson, R. M., 1970. Physical Processes in Geology. Freeman and Company, San Francisco.

Kerkhof, F., 1973. Wave fractographic investigations of brittle fracture dynamics. In: Sih, C.C., (Ed.), Dynamic crack propagation, pp. 3–35. Noordhof, Leyden.

Kulander, B.R., Barton, C.C., Dean, S. C., 1979. The Application of Fractography to Core and Outcrop Fracture Investigations. Report to U.S.D.O.E Morgantown Energy Technology Center, METC, SP-79/3.

Lawn, B.R., Wilshaw, T.R., 1975. Fracture of Brittle Solids. Cambridge University Press, London.

Lockwood, J.P., Moore, J.G., 1979. Regional deformation of the Sierra Nevada, California, on conjugate microfault sets. Journal of Geophysical Research 84, 6041–6049.

Mayo, E.B., 1941. Deformation in the interval Mt. Lyell–Mt. Whitney, California. Geological Society of America Bulletin 94, 563–575.

Mecholsky, J.J., Freiman, S.W., 1979. Determination of fracture mechanics parameters through fractographic analysis of ceramic. In: Freiman, S.W., (Ed.), Fracture Mechanics Applied to Brittle Materials, pp. 136–150. American Society for Testing and Materials, Special Technical Publication, Philadelphia, 78.

Olson, J.E., 1993. Joint pattern development: effects of subcritical crack growth and mechanical crack interaction. Journal of Geophysical Research 98, 12, 251–12, 265.

Peng, S., 1970. Fracture and failure of Chelmford Granite. unpublished Ph.D. thesis. Stanford University, Stanford, U.S.A.

Pollard, D.D., Segall, P., Delaney, P.T., 1982. Formation and interpretation of dilatant échelon cracks. Geological Society of America Bulletin 93, 1291–1303.

Preston, F.W., 1931. The propagation of fissures in glass and other bodies with special reference to the split-wave front. Journal of American Ceramics Society 1, 419–427.

Randall, P.N., 1966. Plain strain crack toughness testing of high strength metallic materials. American Society for Testing and Materials, Special Technical Publication 410, 88–129.

Segall, P., McKee, E.H., Martel, S.J., Turrin, B.D., 1990. Late Cretaceous age of fractures in the Sierra Nevada batholith, California. Geology 18, 1248–1251.

Segall, P., Pollard, D.D., 1983. Joint formation in granitic rock of the Sierra Nevada. Geological Society of America Bulletin 94, 563–575.

Sommer, E., 1969. Formation of fracture "lances" in glass. Engineering Fracture Mechanics 1, 539–546.

Twidale, C.R., 1973. On the origin of sheet jointing. Rock Mechanics 5, 163–187.

Twiss, R. J. and Moores, E. M. (1992) Structural Geology. Freeman, New York.

White, W.S., 1946. Rock-bursts in the granite quarries at Barre, Vermont. U.S. Geological Survey, Circular, 13.

Wiederhorn, S.M., Johnson, H., Diness, A.M., Heuer, A.H., 1974. Fracture of glass in vacuum. Journal of American Ceramics Society 57, 336–341.

Woodworth, J.B., 1895. Some features of joints. Science 2, 903–904.

Yukawa, S., Timo, D. P. and Rubio, A. (1969) Fracture design practices for rotating equipment. In Fracture, ed. H. Liebowitz, pp. 65–157. Academic Press, New York.